# Reduction of Aflatoxin B1 Dialdehyde by Rat and Human Aldo-keto Reductases

**ARTICLE** *in* CHEMICAL RESEARCH IN TOXICOLOGY · MAY 2001

Impact Factor: 3.53 · DOI: 10.1021/tx010005p · Source: PubMed

# Reduction of Aflatoxin $B_1$ Dialdehyde by Rat and Human Aldo-keto Reductases

F. Peter Guengerich,*[,†,‡] Hongliang Cai,[†,‡,§] Michael McMahon,[∥] John D. Hayes,[∥] Thomas R. Sutter,[⊥] John D. Groopman,[#] Zhengwu Deng,[▽] and Thomas M. Harris[‡,▽]

*Departments of Biochemistry and Chemistry and Center in Molecular Toxicology, Vanderbilt University, Nashville, Tennessee 37232-0146, Biochemical Research Centre, Ninewells Hospital and Medical School, University of Dundee, Dundee DD1 9SY, Scotland, United Kingdom, W. Harry Feinstone Center for Genomic Research, University of Memphis, Memphis, Tennessee 38152, and Department of Environmental Health, School of Public Health, Johns Hopkins University, Baltimore, Maryland 21205*

*Received January 9, 2001*

Oxidation of the mycotoxin aflatoxin (AF) $B_1$ yields the 8,9-epoxide, which nonenzymatically hydrolyzes rapidly to a dihydrodiol that in turn undergoes slow, base-catalyzed ring opening to a dialdehyde [Johnson, W. W., Harris, T. M., and Guengerich F. P. (1996) *J. Am. Chem. Soc.* **118**, 8213−8220]. $AFB_1$ dialdehyde does not bind to DNA but can react with protein lysine groups. One enzyme induced by cancer chemopreventive agents is $AFB_1$ aldehyde reductase (AFAR), which catalyzes the NADPH-dependent reduction of the dialdehyde to a dialcohol. $AFB_1$ dialdehyde is known to convert nonenzymatically to $AFB_1$ dihydrodiol at neutral pH, and we reinvestigated the enzymatic reaction by preparing $AFB_1$ dialdehyde at pH 10 and then used this to initiate reactions (at neutral pH) with rat and human AFAR isozymes. Two monoalcohols were identified as products, and their identities were established by $NaB^2H_4$ reduction, chemical cleavage, and mass spectrometry. The monoalcohol corresponding to reduction at C-8 formed first in reactions catalyzed by either the rat or the human AFAR. This C-8 monoalcohol was further reduced to $AFB_1$ dialcohol by AFAR. The other monoalcohol (C-6a) was formed but not reduced to the dialcohol rapidly. Steady-state kinetic parameters were estimated for the reduction of $AFB_1$ dialdehyde by rat and human AFAR to the monoalcohols. The apparent $k_{cat}$ and $K_m$ values were not adequate to rationalize the observed $\Delta A_{340}$ spectral changes in a kinetic model. Simulation fitting was done and yielded parameters indicative of greater enzyme efficiency. A survey of 12 human liver cytosol samples showed a variation of 2.3-fold in AFAR activity. Rats treated with $AFB_1$ excreted the dialcohol and a monoalcohol in urine. The results of these studies are consistent with a role of (rat and human) AFAR in protection against $AFB_1$ toxicity.

## Introduction

Aflatoxin (AF)[1] $B_1$ is produced by several molds that infest peanuts and cereal grains (*2*−*4*). The material was first isolated following an episode involving the accidental poisoning of turkeys in the United Kingdom (*5*). Subsequently, this mycotoxin was demonstrated to be a strong mutagen and carcinogen in experimental animal models (*3*, *6*) and epidemiology supports a role in human liver cancer (*7*, *8*). $AFB_1$ also shows acute toxicity in animals at high doses (*3*, *9*) and has been of interest because of potential use in chemical warfare (*10*).

$AFB_1$ is not reactive per se; all of its biological interactions can be understood in a pathway involving $AFB_1$ 8,9-epoxide (Scheme 1). The enzymes involved in this pathway are very important in determining the biological effects of exposure to the mycotoxin. We have systematically examined kinetics of individual steps of Scheme 1, both nonenzymatic and enzymatic, particularly with the relevant human enzymes (*11*). The oxidation of $AFB_1$ is catalyzed by P450s, particularly (human) P450 3A4 (*12*, *13*). P450 3A4 yields only the exo isomer; other P450s can yield both the exo and endo epoxides, with lower catalytic efficiency (*11*, *13*−*15*). Only the exo epoxide reacts with DNA, and this acid-catalyzed reaction has been characterized in detail (*16*, *17*). Both the exo and endo epoxides are substrates for GSH conjugation catalyzed by GSH transferases (GSTs), and rates have been

* To whom correspondence should be addressed. Department of Biochemistry and Center in Molecular Toxicology, Vanderbilt University School of Medicine, Nashville, TN 37232-0146. Phone: (615) 322-2251. Fax: (615) 322-3141. E-mail: guengerich@toxicology.mc.vanderbilt.edu.

† Department of Biochemistry, Vanderbilt University.

‡ Center in Molecular Toxicology, Vanderbilt University.

§ Present address: Pfizer Global R & D, 2800 Plymouth Road, Ann Arbor, MI 48105.

∥ University of Dundee.

⊥ University of Memphis

# Johns Hopkins University.

▽ Department of Chemistry, Vanderbilt University.

[1] Abbreviations: AF, aflatoxin; AFAR, aflatoxin $B_1$ aldehyde reductase [rAFAR = rat AFAR (AKR7A1), hAFAR1 = human AFAR 1 (AKR7A2), hAFAR2 = human AFAR2 (AKR7A3) (*1*)]; HEPES, *N*-(2-hydroxyethyl)piperazine-*N*′-(2-ethanesulfonate); CHES, 2-(*N*-cyclohexylamino)ethanesulfonate; MES, 2-(*N*-morpholino)ethanesulfonate; MOPS, 3-(*N*-morpholino)propanesulfonate; tricine, *N*-tris(hydroxymethyl)methylglycine; bicine, *N*,*N*-bis(2-hydroxyethyl)glycine; GST, GSH transferase; ESI, electrospray ionization.

10.1021/tx010005p CCC: $20.00 
Published on Web 05/10/2001

**Scheme 1. Major Steps in $AFB_1$ Metabolism**

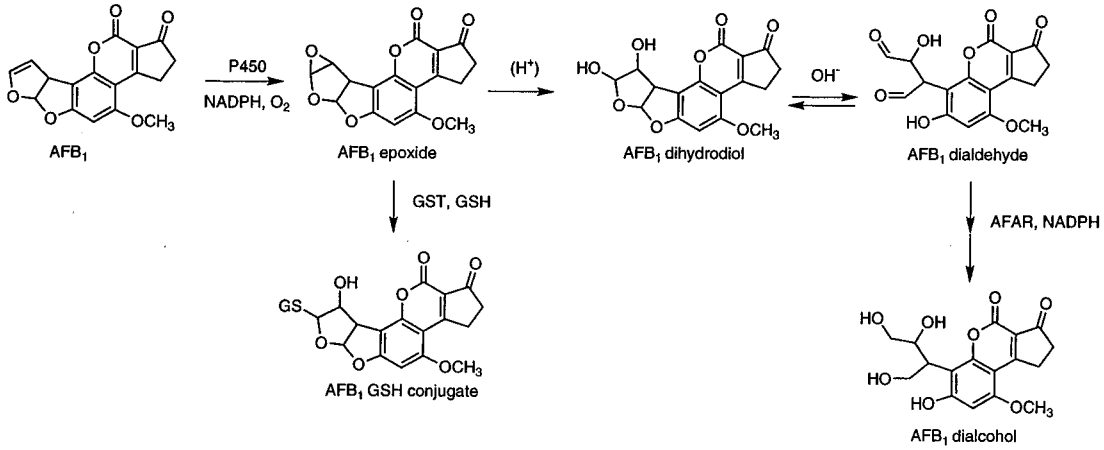


estimated for rat and human GSTs (*18*, *19*). $AFB_1$ epoxides undergo rapid hydrolysis to the dihydrodiol, acid-catalyzed at pH <4 (*20*). Only slight enhancement of this rapid reaction ($k = 0.7\ s^{-1}$ at 23 °C) is seen with rat (but not human) epoxide hydrolase (*21*). $AFB_1$ dihydrodiol undergoes base-catalyzed ring opening to $AFB_1$ dialdehyde, which is a reversible reaction with an effective $pK_a$ of ~8.2 (*20*).

$AFB_1$ dialdehyde is of interest because it appears to be able to react with proteins but not DNA. Both the exo and endo epoxides yield $AFB_1$ dihydrodiols and $AFB_1$ dialdehydes. The dialdehyde cannot be very genotoxic because the endo epoxide (which is converted to the dihydrodiol and the dialdehyde) is not genotoxic (*16*). Formation of protein adducts is believed to derive from the dialdehyde and a Lys adduct has been characterized (*22*). A rat aldo-keto reductase has been characterized as reducing $AFB_1$ dialdehyde to $AFB_1$ dialcohol with NADPH (Scheme 1) and termed $AFB_1$ aldehyde reductase (AFAR). This enzyme was discovered because it is markedly induced in the liver by chemopreventive agents, such as ethoxyquin and dithiolethiones, that reduce $AFB_1$ toxicity (*23*). AFAR is proposed to play a role in resistance to $AFB_1$ toxicity (*24*). However, it is known that ethoxyquin and dithiolethiones also induce GSTs as well as other enzymes, and therefore, the exact role of AFAR in protection against $AFB_1$ is not completely clear. Subsequently, two human aldo-keto reductases that share >75% identity with rAFAR have been identified and found to reduce $AFB_1$ dialdehyde. These have been designated hAFAR1 (AKR7A2) and hAFAR2 (AKR7A3) (*23*, *25*, *26*). Recently, a second rat AFAR has been isolated (*27*) and cloned (*28*) [termed rAFAR2 by Kelly et al. (*27*) and AIAR by Nishi et al. (*28*)]. The exact functional relationship between the two human and the two rat reductases is not presently clear.

In some of our earlier kinetic investigations, we found that the conversion of $AFB_1$ dihydrodiol to the dialdehyde is a relatively slow process at neutral pH (*20*) and considered the chemical steps in the AFAR reaction, as well as the important parameters in the process. Because of the nature of the chemical kinetics (*20*), studies in which $AFB_1$ epoxide and dihydrodiol (of unknown stereochemistry) are produced by liver microsomes cannot be used to estimate steady-state kinetic parameters for the reduction reaction.

With our previous knowledge of the kinetics of reactions involving $AFB_1$, we prepared $AFB_1$ dialdehyde and reduced it with rAFAR1 (AKR7A1) and hAFAR2 (AKR7A3) under conditions where ring closure was minimized. The sites of reduction were identified and the results are rationalized in kinetic schemes.

## Experimental Procedures

**Caution!** $AFB_1$ exo-8,9-epoxide is a potent mutagen (*16*) and probable carcinogen and should be handled only with gloves and other appropriate precautions. Glassware and unused samples should be destroyed with bleach (HOCl).

**Chemicals.** $AFB_1$ *exo*-8,9-epoxide was synthesized from $AFB_1$ (Sigma Chemical Co., St. Louis, MO) by oxidation with either dimethyldioxirane (*29*) or *m*-chloroperbenzoic acid (*30*) and recrystallized from $CHCl_3/(CH_3)_2CO$ (*29*). The material was stored desiccated at −20 °C. Samples were dissolved in dry $CH_3CN$ and aliquots were hydrolyzed to the dihydrodiol by dilution in 20 mM sodium 2-(*N*-cyclohexylamino)ethanesulfonate (CHES, pH 10.0). Dilutions were made in pH 5 buffer in order to estimate concentrations using $\epsilon_{360} = 21\ 800\ M^{-1}\ cm^{-1}$ (*31*). Stock alkaline samples (20 mM sodium CHES, pH 10.0) were stored ≤3 days at −20 °C.

**Enzymes.** *Escherichia coli* recombinant rAFAR1 (oligo-His version) was prepared as described (*32*). The catalytic activity (following shipping from Dundee to Nashville) was confirmed using reduction activity with 4-nitrobenzaldehyde (*33*). Oligo-His-tagged rAFAR1 and hAFAR2 were prepared as described (*23*).

**Spectroscopy and HPLC.** UV spectra and transient absorbance readings were made with a Cary 14/OLIS spectrophotometer (On-Line Instrument Systems, Bogart, GA). HPLC was done using a Spectra-Physics 8700 pumping system (ThermoSeparations, Piscataway, NJ) with a 6.2 × 80 mm Zorbax octylsilane (C8) column (3 μm, Mac-Modd, Chadds Ford, PA) and a solvent gradient consisting of (solvent A) $H_2O/CH_3CN/CH_3CO_2H$, 95−5−0.1, v/v/v and (solvent B) $CH_3CN/H_2O$, 90−10, v/v. Typically the flow rate was 2.0 mL $min^{-1}$ and the gradient schedule was $t = 0$, 95% A/5% B, v−v; $t = 12$ min, 60% A, 40% B, v−v; $t = 14$ min, 35% A, 65% B, v−v; $t = 15$ min, 95% A, 5% B, v−v. The eluent passed through a ThermoSeparation Products 6000 detector equipped with a rapid-scanning monochromator (ThermoSeparation Products, Piscataway, NJ) and a McPherson FL-750BX spectrofluorimeter (McPherson, Acton, MA) [$\lambda_{exitation}$ 360 nm, $\lambda_{emission}$ (filter) 440 nm]. UV spectra were recorded, with subtraction of solvent absorbance as necessary. When spectra of HPLC peaks were recorded at neutral pH, a Pharmacia P-500 pump (Pharmacia, Piscataway, NJ) was used with a Valvco mixer (Valvco, Houston, TX) to add 0.5 M potassium HEPES buffer (pH 7.7) to the eluent (buffer flow 1.0 mL $min^{-1}$, HPLC solvent flow 2.0 mL $min^{-1}$), yielding a final pH of 7.6 in the detector line.

MS was carried out with $AFB_1$ products generated from in vitro experiments at the Vanderbilt University facility, using a

Finnigan TSQ 7000 triple quadrupole mass spectrometer (Finnigan MAT, Sunnyvale, CA) operating in the positive ion mode with an electrospray needle voltage of 4.5 kV. $N_2$ was used as the sheath gas (70 psi) to assist nebulization and as the auxiliary gas (10 psi) to assist with desolvation. The stainless steel capillary was heated to 250 °C. The tube lens and the heated capillary were operated at 75 and 20 V, respectively, and the electron multiplier was set at 2000 V. HPLC conditions (YMC C18 ODS-AQ, 5.0 $\mu$m, 2.0 × 150 mm) were as follows: flow rate, 0.2 mL min$^{-1}$; solvent A, 0.1% $CH_3CO_2H$ in 95% $H_2O$ and 5% $CH_3OH$ (v/v); solvent B, 0.1% $CH_3COOH$ in 50% $H_2O$ and 50% $CH_3OH$ (v/v); at $t = 0$ min, 100% A and 0% B; $t = 5$ min, 0% A and 100% B; $t = 11$ min, 0% A and 100% B; $t = 13$ min, 100% A and 0% B.

NMR spectra were recorded at 400.13 MHz with a Bruker AM-400 instrument (Bruker, Billerica, MA) in the Vanderbilt University facility.

**Human Liver Samples.** Twelve human liver samples were obtained from organ donors through Tennessee Donor Services (Nashville, TN). Available details about age, causes of death, and drugs used is included in the Supporting Information. Cytosolic functions were prepared as described (*34*) and dialyzed twice vs 30 volumes of 0.10 M potassium phosphate buffer (pH 7.4) containing 1 mM EDTA (3 h then 14 h at 4 °C) in order to remove tris(hydroxymethyl)aminomethane buffer, which could react with the $AFB_1$ aldehydes. Protein concentrations were estimated using a bicinchoninic acid assay (BCA, Pierce, Rockford, IL).

Assays of $AFB_1$ dialdehyde reduction were performed by incubating cytosol (10 mg protein mL$^{-1}$), 83 mM potassium phosphate buffer (pH 7.4), and an NADPH-generating system (*34*) in a total volume of 594 $\mu$L at 37 °C. Reactions were started with the addition of 6 $\mu$L of 7.0 mM $AFB_1$ dialdehyde (in 25 mM sodium CHES buffer, pH 10.0). After 60 s, reactions were quenched with the addition of 200 $\mu$L of 17% $HClO_4$, chilled on ice, and centrifuged (10 min, $3 \times 10^3 \times g$) to precipitate protein and $KClO_4$. HPLC (vide supra) was used to separate products, with quantitation using the fluorescence detector ($F_{360/440}$). Results are expressed as means of results of duplicate assays.

**Synthesis of $AFB_1$ Dialcohol.** $AFB_1$ *exo*-8,9-epoxide (~1 mg) was dissolved in 2.9 mL of $CH_3CN$, followed by the addition of 2.9 mL of sodium CHES (pH 10.0, 20 mM). After 5 min, a solution of $NaBH_4$ in *N*,*N*-dimethylformamide (0.43 mL, 89 mM) was added and the reaction mixture was mixed using a vortex device. After 30 min, $CH_3CN$ was removed in vacuo and the product was purified by semipreparative HPLC, yield ~85%. HPLC conditions (YMC-Pack ODS-AQ octadecylsilane column, 10 × 250 mm, YMC Corp., Wilmington, NC) were as follow: flow rate, 2.5 mL min$^{-1}$; solvents and gradients as described for analytical systems (vide infra). $^1$H NMR ($d_6$-$Me_2SO$) (*24*) $\delta$ 2.43 (t, 2H, H-2, see ref *20* for numbering), 3.20 (d, 2H, H-8a), 3.25 (t, 2H, H-3), 3.48 (m, 2H, H-9), 3.60 (q, 1H, H-9), 3.84 (s, 3H, OC*H*$_3$), 4.05 (q, 1H, H-8b), 6.18 (s, 1H, H-5); MS *m*/*z* 351.11 ($MH^+$).

**Analysis of Monoalcohols.** $AFB_1$ monoalcohol [1−12 nmol, as estimated from $\epsilon_{360} \approx 21\,800$ M$^{-1}$ cm$^{-1}$ (*31*) and obtained from enzymatic reaction following semipreparative HPLC] was dissolved in 150 $\mu$L of $CH_3CN$. The solution was transferred into a reaction vial and evaporated to dryness under a stream of $N_2$. Subsequently, $CH_3CN$ (10 $\mu$L) and 10 $\mu$L of 20 mM sodium CHES (pH 10.0) were added to the reaction vial followed by an addition of a solution of $NaB^2H_4$ in *N*,*N*-dimethylformamide (5 $\mu$L, 89 mM). After 40 min reaction, the product ($AFB_1$ dialcohol) was purified by semipreparative HPLC (vide supra).

$AFB_1$ dialcohol (recovered from $NaB^2H_4$ reduction) was dissolved in 0.11 mL of 0.10 M potassium phosphate (pH 7.4). A solution of $NaIO_4$ (20 mM in $H_2O$, 10 $\mu$L) was added. HPLC/MS analysis was performed after 5 min of reaction time.

**Kinetics and Reaction Modeling.** Changes in $A_{340}$ were recorded at 37 °C in a Cary 14/OLIS instrument, saved as ASCII files, and converted to Cricket Graph and then Word text files for use with DYNAFIT software (all done on a Macintosh G3 computer, Apple Computer, Cupertino, CA). DYNAFIT is a fitting and simulation system used to analyze kinetic data (*35*) (available from Dr. P. Kuzmic at the University of Wisconsin <http://www.biokin.com/>).

The mechanism used for the analysis of the $A_{340}$ results, as written for DYNAFIT, was

| | |
|---|---|
| $S \leftrightarrow X$ | $k_1\ k_{-1}$ |
| $E + S \leftrightarrow ES$ | $K_2$ dissoc |
| $ES + H \leftrightarrow ESH$ | $K_3$ dissoc |
| $ESH \rightarrow EPN$ | $k_4$ |
| $ESH \rightarrow EQN$ | $k_5$ |
| $EPN \leftrightarrow EP + N$ | $K_6$ dissoc |
| $EP \leftrightarrow E + P$ | $K_7$ dissoc |
| $EP + H \leftrightarrow EPH$ | $K_8$ dissoc |
| $EPH \leftrightarrow ERN$ | $k_9$ |
| $ERN \leftrightarrow ER + N$ | $K_{10}$ dissoc |
| $ER \leftrightarrow E + R$ | $K_{11}$ dissoc |

where S = $AFB_1$ dialdehyde ($\epsilon_{340} = 0.013$), X = $AFB_1$ dihydrodiol ($\epsilon_{340} = 0.018$), E = rAFAR ($\epsilon_{340} = 0$), P = monoalcohol **2** ($\epsilon_{340} = 0.018$), Q = monoalcohol **1**, R = dialcohol product ($\epsilon_{340} = 0.0022$), H = NADPH ($\epsilon_{340} = 0.0062$), and N = $NADP^+$ ($\epsilon_{340} = 0$), with the extinction coefficients expressed in $\mu$M$^{-1}$ cm$^{-1}$. Initial concentrations were E = 3.4 $\mu$M, S = 57 $\mu$M, and H = 50 $\mu$M.

**Animals, Diets, and Treatments.** Male Fischer 344 rats (100−150 g; Harlan, Indianapolis, IN) were housed under controlled conditions of temperature, humidity, and lighting in the facility at Johns Hopkins University. Food and water were available ad libitum. Purified diet of the AIN-76A formulation (Teklad, Madison, WI) (without the recommended addition of 0.02% ethoxyquin) was used, and fresh diet was provided to animals at least every other day. Rats were acclimated to the AIN-76A diet for one week before beginning the experiments. Six rats were dosed for 10 consecutive days with 25 $\mu$g of $AFB_1$ in 100 $\mu$L of $Me_2SO$ by i.p. injection. These animals were housed in metabolic cages and urine was collected daily on dry ice.

**Identification and Characterization of AF Metabolites In Urine By ESI-LC/MS/MS.** Rat urine samples were first adjusted to an acidic pH using 1 M $NH_4HCO_2$, pH 4.5, and then the total volume was increased to 10 mL with water. The sample was spiked with 2 ng of $AFB_2$ (Sigma), as an internal standard, and loaded onto a preprimed Waters Oasis HLB 3 mL column (Waters Corp., Milford, MA). The preparative column was sequentially washed with 10 mL of $H_2O$ and 10 mL of 5% $CH_3OH$ in $H_2O$ (v/v), and the AFs were eluted from the column with 3 mL of 100% $CH_3OH$. The $CH_3OH$ was evaporated using a ultrahigh purity Ar stream, and the dried fraction was reconstituted using 1−2 mL of 10 mM potassium phosphate buffer (pH 7.4) containing 0.15 M NaCl and loaded onto an AF-specific preparative monoclonal antibody immunoaffinity column (*36*) at a flow rate of 0.3 mL min$^{-1}$. The affinity column was washed twice with 5 mL of 20 mM potassium phosphate buffer (pH 7.4) containing 0.15 M NaCl and once with 10 mL of $H_2O$ to remove nonspecifically bound materials. AF derivatives were then eluted from the immunoaffinity column with 2 vol of 60% $Me_2SO$ in $H_2O$ (v/v) followed by another 2 vol of $H_2O$. The $Me_2SO$ and $H_2O$ eluates were combined, diluted with 8 mL of $H_2O$ and then applied to another pre-primed Waters Oasis HLB 3 mL column. The Oasis column was washed with 10 mL of $H_2O$ and 10 mL of 5% $CH_3OH$ in $H_2O$ (v/v) to remove $Me_2SO$. AF derivatives were eluted with 3 mL of 100% $CH_3OH$. The

$CH_3OH$ was evaporated under an Ar stream (vide supra) and then reconstituted in 1% $CH_3CO_2H$ in $H_2O$ (v/v) for analysis by LC/MS-ESI. Using rat urine samples spiked with known amounts of $AFB_2$, 85−90% recovery was estimated.

A Thermoquest LCQ LC/MS system was used for LC/MS-ESI and LC/MS/MS-ESI on the immunoaffinity-processed urine to identify and quantify the AF derivatives at the Johns Hopkins University facility. A Thermal Systems Products HPLC was used to provide constant flow of 100 $\mu$L $min^{-1}$ to a YMC ODS J-sphere M-80 column (1.0 × 250 mm). For these analyses, gradients using combinations of $CH_3CN$ and $CH_3OH$ were used to affect separation of the AFs. The buffer used in all the separations was 1% $CH_3CO_2H$ in $H_2O$ (v/v), with the HPLC column temperature maintained at 55 °C.

## Results

**Experimental Design. General.** When $AFB_1$ epoxide is hydrolyzed, the dihydrodiol, which cannot be reduced by AFAR, undergoes a slow base-catalyzed (nonenzymatic) opening to the dialdehyde, which converts back to the dihydrodiol at neutral or acidic pH (Scheme 1). We examined the ability of AFAR to catalyze the reduction of intermediate aldehyde forms. $AFB_1$ *exo*-8,9-epoxide was converted to $AFB_1$ dihydrodiol by hydrolysis in 20 mM sodium CHES buffer at pH 10, at which it exists as the dialdehyde form-phenolate anion. Aliquots were diluted into neutral buffer containing AFAR and NADPH to initiate reactions.

**Preliminary Analysis of Reduction Products.** An aliquot of a basic solution (pH 10.0) of $AFB_1$ dialdehyde was added to rAFAR1 at pH 7.4, in the presence of NADPH. After 60 s the reaction was quenched by the addition of $HCO_2H$, which stopped catalysis by rAFAR1 and converted nonreduced $AFB_1$ dialdehyde forms to the dihydrodiol (*20*). HPLC analysis [using a modification of the procedure of Judah et al. (*24*)] showed the presence of two major peaks, designated **1** ($t_R$ 6.7 min) and **2** ($t_R$ 7.2 min) (Figure 1A).[2] Peak **4** ($t_R$ 10.4 min) was observed in controls devoid of either rAFAR1 or NADPH and is the dihydrodiol. Only peak **4** was observed when the $AFB_1$ dialdehyde solution was mixed with the pH 7.4 sodium *N*-(2-hydroxyethyl)piperazine-*N*′-(2-ethanesulfonate) (HEPES) buffer for 5 min and rAFAR1 prior to addition of NADPH (Figure 1B). The peak at $t_R$ 9.7 min was subsequently found to have the same UV and mass spectra as the dihydrodiol (**4**) and is considered to be either the dialdehyde or other isomers (*20*) because of the broad nature; this peak had variable contribution in different experiments and is sometimes designated **4a**.

**Characterization of rAFAR1 Reduction Activity.** In preliminary experiments, the HPLC analysis of $AFB_1$ dialdehyde reduction products (60 s incubation) following addition of basic dialdehyde to rAFAR1 showed optimal formation of peak **2** [and also peak **1** (and **3**)] at pH 7.4.[3]

The time course of the appearance of the individual HPLC peaks (Figure 2) indicates clearly that peak **2** is formed first and then decreases. Peak **1** formation was linear with time. Peak **3** showed a lag, which would be expected for dialcohol. The amount of the dihydrodiol, peak **4**, decreases with time. These results are suggestive

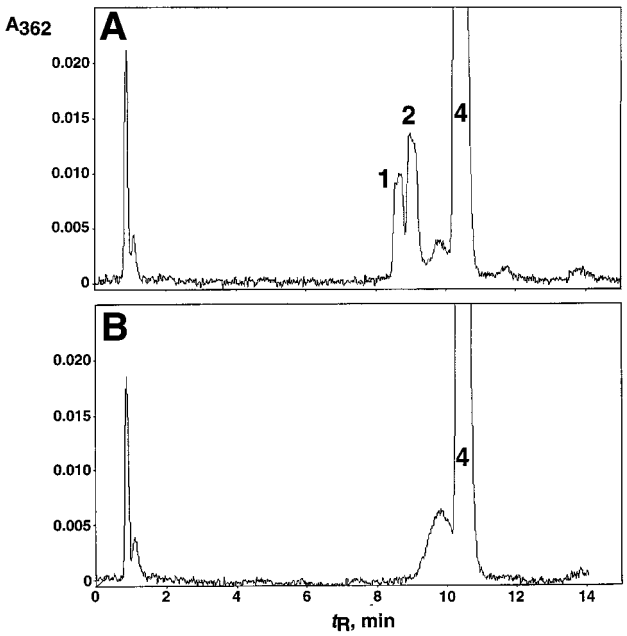


**Figure 1.** HPLC/UV analysis of $AFB_1$-dialdehyde reduction products. (A) $AFB_1$ dialdehyde (15 $\mu$L of a solution in 20 mM sodium CHES, pH 10.0, prepared from $AFB_1$ *exo*-8,9-epoxide) was added (final addition, to 50 $\mu$M) to a 200 $\mu$L mixture of 3.4 $\mu$M rAFAR1, 50 mM potassium HEPES (pH 7.4), and a premixed NADPH-generating system (*34*). Incubation proceeded for 60 s at 37 °C, when the reaction was quenched by the addition of 40 $\mu$L conc $HCO_2H$ and chilled on ice. A 200 $\mu$L aliquot was injected into the HPLC system described under Experimental Procedures. (B) The components were as in part A except that rAFAR1 and $AFB_1$ dialdehyde were mixed with potassium HEPES (pH 7.4) for 5 min before the reaction was initiated with NADPH.

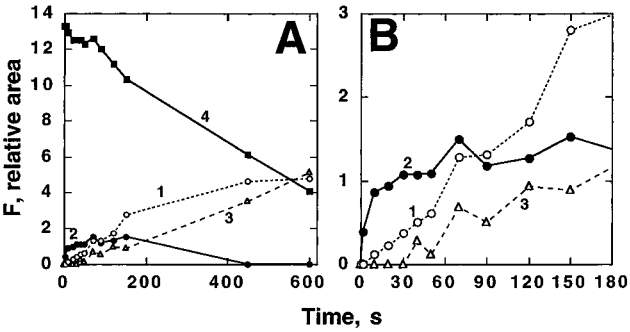


**Figure 2.** Time course of peaks **1**−**4** from reaction of $AFB_1$ dialdehyde with rAFAR1 and NADPH. Quantitation was done on the basis of fluorescence of the HPLC peaks (peak area), with the assumption that all of the compounds have identical fluorescence. The plot of product formation is expanded in part B. **1** (○), **2** (●), **3** (△), **4** (■).

of a relationship in which the peak **2** monoalcohol is further reduced to the dialcohol and the peak **1** monoalcohol is relatively stable and is only converted slowly to the dialcohol.

**Spectral Analysis of Products.** Peaks **1**−**3** had UV spectra very similar to **4** at acidic pH (pH 2.6 in HPLC solvent), with $\lambda_{max} \sim 360$ nm (Figure 3). At pH 7.6 the spectra of peaks **1**, **2**, and **4** were identical to those observed at acid pH, but the spectrum of **3** had a $\lambda_{max}$ at 395 nm and is judged to be the dialcohol, based on comparison with the spectra of Judah et al. (*24*).

HPLC/MS of the sample (Figure 4) yielded the expected $MH^+$ at *m*/*z* 347 for peak **4** as the dihydrodiol (also *m*/*z* 347 for preceding shoulder, **4a**). Peak **3** is the dialcohol

[2] Peak **3** (vide infra) did not appear until after 60 s.

[3] Buffers used included pH 6.0 sodium 1-(*N*-morpholino)ethanesulfonate (MEPS), pH 6.5 sodium MEPS, pH 7.0 sodium 3-(*N*-morpholino)propanesulfonate (MOPS), pH 7.5 sodium HEPES, pH 8.0 sodium *N*-tris(hydroxymethyl)methylglycine (tricine), and pH 8.5 sodium *N*,*N*-bis(2-hydroxyethyl)glycine (bicine).

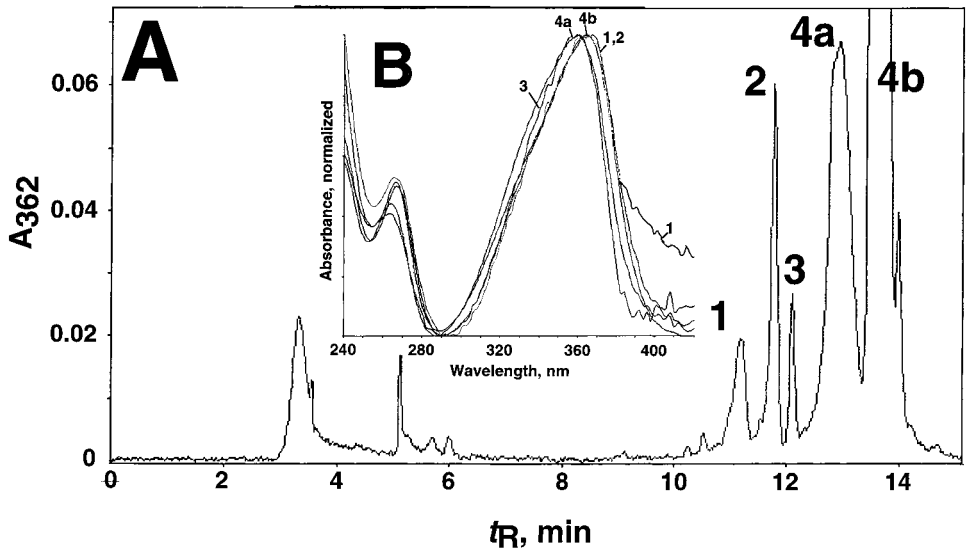


**Figure 3.** HPLC and UV spectra of rAFAR1 reduction products from $AFB_1$ dialdehyde. (A) A preparative incubation was done using the components described in Figures 1 and 1.0 mL of the mixture ($t = 60$ s) was analyzed using a 10 × 250 mm octadecylsilane column (5 $\mu$m) and the same solvent gradient (flow 4.0 mL $min^{-1}$). (B, inset) Spectra are shown; $\lambda_{max}$ values for the indicated peaks were **1**, 366 nm; **2**, 367 nm; **3**, 361 nm; **4a**, 360 nm; and **4b**, 365 nm.

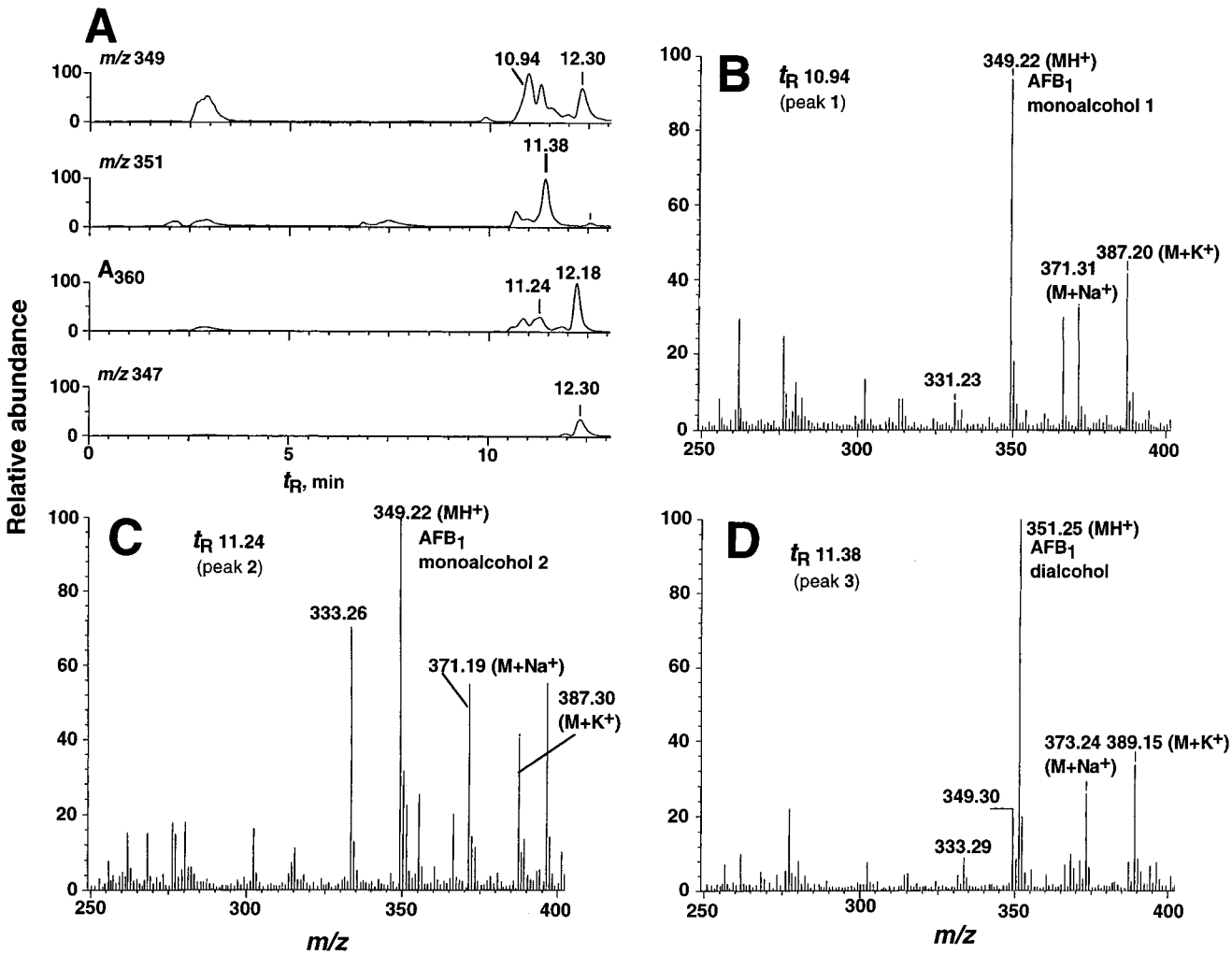


**Figure 4.** HPLC/MS analysis of $AFB_1$ dialdehyde reduction products. The reaction products described in Figure 3 were analyzed by HPLC/MS (ESI) as described in the Experimental Procedures. (A) Selected *m/z* and $A_{360}$ traces, with the latter being used to compare patterns with previous experiments (Figures 1 and 3). (B−D) Full spectra of peaks eluting at $t_R$ (B) 10.94 min, (C) 11.24 min, and (D) 11.38 min.

product, as judged by its $MH^+$ at *m/z* 351. Peaks **1** and **2** are monoalcohol reduction products of the dialdehyde on the basis of their mass spectra ($MH^+$ 349).

**$NaBH_4$ Reduction Products.** Treatment of $AFB_1$-dialdehyde with 0.5 equivalent of $NaBH_4$ (based on $H^-$ ions) for 30 s at 0 °C yielded HPLC peak **1** in ∼10×

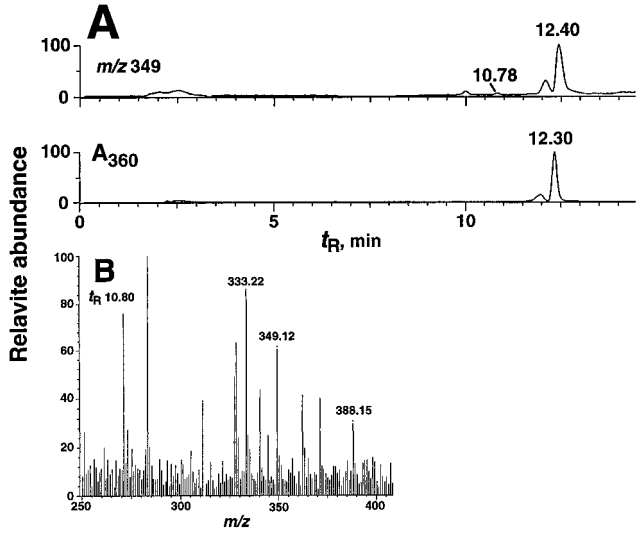


**Figure 5.** (A) HPLC/MS of $NaBH_4$ reduction products of $AFB_1$ dialdehyde. $AFB_1$ dialdehyde (7.3 nmol) was treated with 1.0 nmol of $NaBH_4$ in 20 mM potassium HEPES for 30 s at 0 °C. The $t_R$ values are displaced about 0.1 min later than in Figure 4. (B) Full spectrum of peak at $t_R$ 10.80 min ($MH^+$ at *m/z* 349).

greater amount than peak **2**, as judged by HPLC fluorescence assays (results not presented) at either pH 10 or directly after adjustment to pH 7.4. HPLC/MS analysis also showed that peak **1** was the major product (Figure 5).

**Identification of Monoalcohols 1 and 2.** The strategy for defining the positions of reduction of $AFB_1$ dialdehyde to yield peaks **1** and **2** is presented in Scheme 2. Reduction of the monoalcohols with $NaB^2H_4$ places $^2H$ in the position that is not reduced by rAFAR1. The $NaIO_4$ oxidative HCHO release reaction proceeded quickly with the dialcohol and yielded the putative aldehyde product ($MH^+$ 319). This product was collected and (at acidic pH) had a similar UV spectrum to the dihydrodiol. HCHO was also detected [using the Nash assay (*37*)] and, assuming an $\epsilon_{360}$ of 21 800 $M^{-1}$ $cm^{-1}$ for the coumarin product [as for other $AFB_1$ derivatives (*31*)], the yield of HCHO was 90% of theoretical.

The procedure was used with $NaB^2H_4$ and $NaIO_4$ on the two isolated peaks, **1** and **2** (Figures 1 and 3). Only the product derived from peak **2** contained deuterium (Figure 6). Thus, we conclude that the C-8 position is reduced to a monoalcohol to yield peak **2**; the C-6a position is reduced to yield peak **1** (Scheme 2).

In the course of work with the $NaIO_4$ oxidative HCHO release reaction, we found that the product of the reaction yielded another compound upon standing at neutral pH. This product was separable by HPLC ($t_R$ 11.7 min on HPLC system of Figure 6) and had an $MH^+$ ion at *m/z* 301, indicating a loss of the elements of $H_2O$. We postulate that this compound is the furanocoumarin shown in Scheme 2. Its UV spectrum was quite different from that of the initial $NaIO_4$ product, which resembled $AFB_1$-related compounds (Figure 3), and had $\lambda_{max}$ at 283 and 395 nm. This spectrum has some similarity to that of another isopsoralen, allobergaptene (*38*, *39*). Allobergaptene has $\lambda_{max} = 340$ nm ($\epsilon_{340} = 10\,500$ $M^{-1}$ $cm^{-1}$) (*38*) and the conjugation would be extended by the addition of a cyclopentanone ring. However, a better prediction of the UV spectrum can be made by comparison with the

**Scheme 2. Analysis of Monoalcohol Reduction Products of $AFB_1$ Dialdehyde**

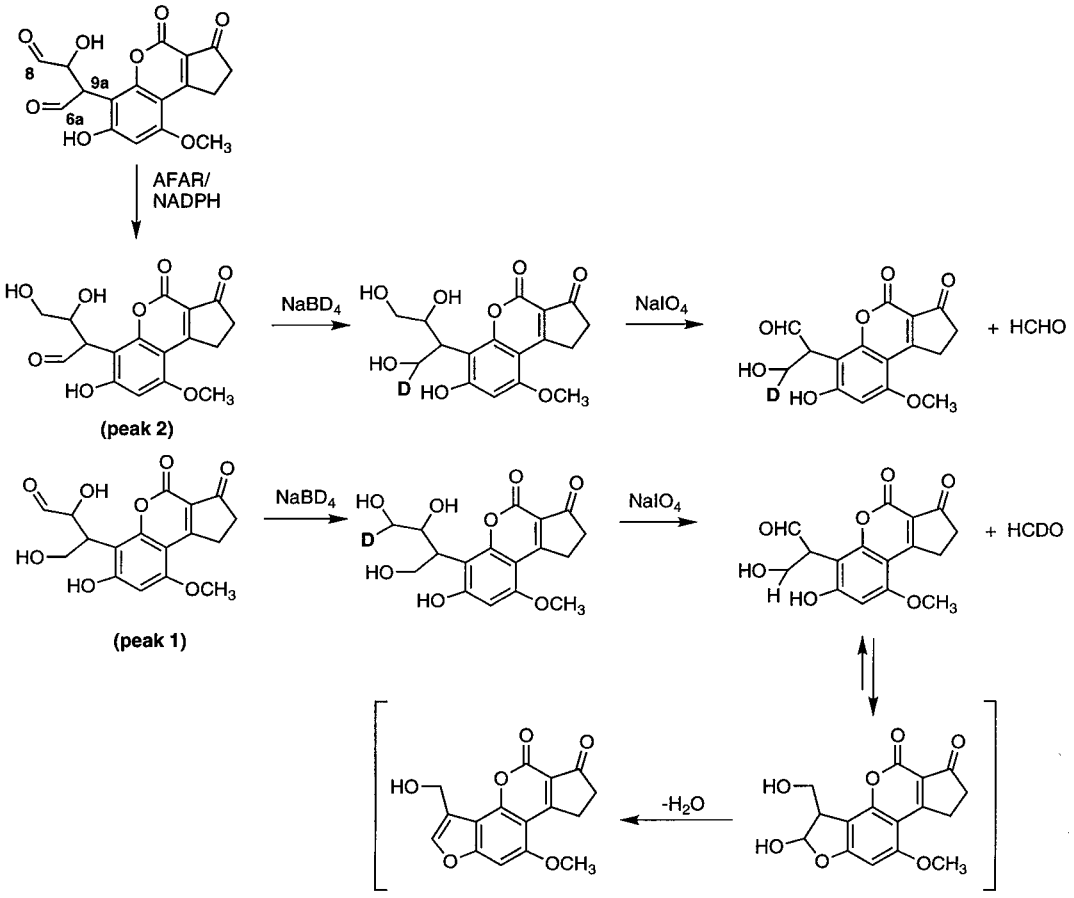

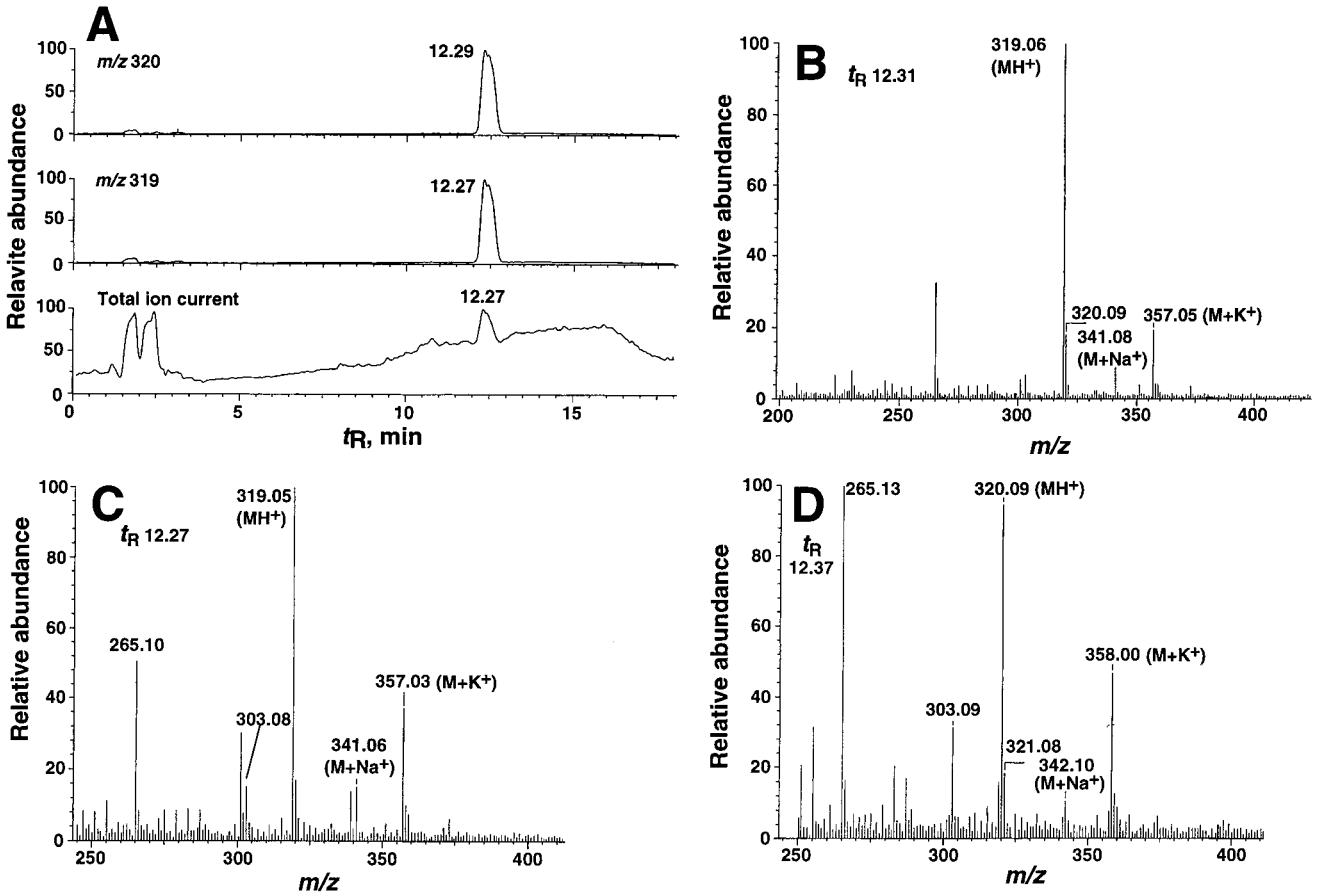


**Figure 6.** Analysis of $AFB_1$ dialcohol $NaIO_4$ oxidation products following treatment of $AFB_1$ monoalcohols with $NaB^2H_4$. The products of a preparative incubation of $AFB_1$ dialdehyde with rat AFAR and NADPH (similar to Figure 1, 4 mL volume) were separated by HPLC. Monoalcohols **1** and **2** were collected from HPLC separately, concentrated to dryness by lyophilization, and reduced with $NaB^2H_4$. The resulting $AFB_1$ dialcohol samples were purified by HPLC and the dialcohol peaks were collected and concentrated by lyophilization. The compounds were treated with $NaIO_4$ for 5 min and the products were analyzed by HPLC/MS, monitoring *m/z* 319 and 320 ($MH^+$) and total ion current. (A) MS ion current traces. These traces demonstrate that only a single peak is found corresponding to each of the anticipated products, and the only other chemicals in the reaction mixture are eluted at the start of the run. (B) Full spectrum of $NaIO_4$ oxidation product of the dialcohol recovered directly from AFAR/NADPH reduction of $AFB_1$ dialdehyde. (C) Full spectrum of peak **1** (recovered from AFAR reduction of $AFB_1$ dialdehyde) treated with $NaB^2H_4$ and $NaIO_4$ as described. (D) Full spectrum of peak **2** (recovered from AFAR reduction of $AFB_1$ dialdehyde) treated with $NaB^2H_4$ and $NaIO_4$ as described.

structure of $AFB_1$ and related compounds ($\lambda_{max} \approx 360$ nm) in which the addition of a double bond to the conjugation system would add ~30 nm (*40*) to give $\lambda_{max} \approx 390$ nm. Precedent for the formation of a benzofuran ring system in such a reaction, including dehydration, is seen in the P450-catalyzed oxidation of the terpene pulegone to menthofuran (*41*). In a separate set of $NaIO_4$ treatments of $NaB^2H_4$-reduced peaks **1** and **2**, in which the $NaIO_4$ reaction proceeded for 30 min, we observed $MH^+$ at *m/z* 301 peak **1** and at *m/z* 302 from peak **2**, confirming the result obtained with the initial products (and demonstrating the retention of the deuterium in the final product).

**Steady-State Kinetic Estimates with Rat and Human AFAR.** Preliminary studies of the hAFAR2-catalyzed reduction of $AFB_1$ dialdehyde indicated that peak **2** was formed in preference to peak **1**, as in the case of rAFAR1 (Figure 2) (results not shown). The formation of the monoalcohols by rAFAR1 and hAFAR2 was examined (HPLC/fluorescence) in 15 s reactions, as a function of the concentration of the dialdehyde substrate (Figure 7). $k_{cat}$ and $K_m$ values were estimated for the formation of the two products (Table 1). Formation of peak **1** by rAFAR1 was not saturating (with respect to substrate),

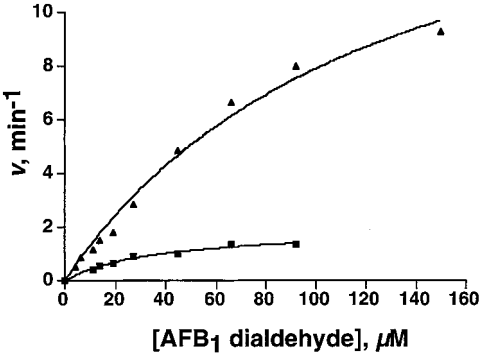


**Figure 7.** Rate of formation of $AFB_1$ monoalcohols by rAFAR1 as a function of $AFB_1$ dialdehyde concentration. Each reaction was done for 15 s and peaks **1** (■) and **2** (▲) were quantified by HPLC/fluorescence measurements.

and the result is expressed as the ratio $k_{cat}/K_m$, an approximation of the tangent to the curve.

**Modeling of Kinetics of Rat AFAR Reduction.** Reductions by AFAR involve the oxidation of NADPH and can be monitored by measuring the decrease in $A_{340}$ (*33*). The reaction with $AFB_1$ dialdehyde is complicated by the (nonenzymatic) increase in $A_{340}$ that occurs when the dialdehyde undergoes conversion to ring-closed forms

**Table 1. Steady-State Kinetic Parameters Measured for Reduction of $AFB_1$ Dialdehyde**

| | product | | | |
|---|---|---|---|---|
| | monoalcohol 1 | | monoalcohol 2 | |
| enzyme | $k_{cat}$ ($min^{-1}$) | $K_m$ ($\mu M$) | $k_{cat}$ ($min^{-1}$) | $K_m$ ($\mu M$) |
| rAFAR1 | *a* | *a* | 12 ± 3 | 109 ± 48 |
| hAFAR2 | 2.0 ± 0.2 | 36 ± 6 | 18 ± 2 | 127 ± 23 |

[a] $k_{cat}/K_m = 0.025\ min^{-1}\ \mu M^{-1}$.

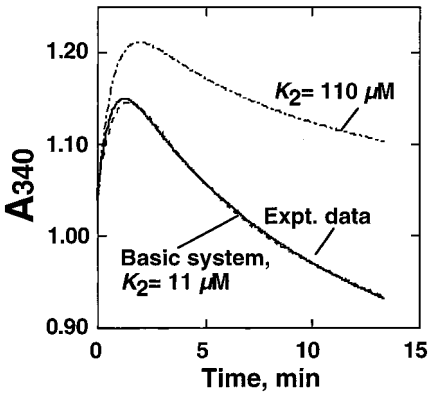


**Figure 8.** Change in $A_{340}$ during reaction of $AFB_1$ dialdehyde with NADPH in the presence of rAFAR1. See Experimental Procedures for DYNAFIT mechanism and concentrations. The experimental trace (- - -) and the simulated fits are indicated. For the fit shown (indicated "$K_2$ = 3 $\mu$M"), $k_1$ = 1.2 $min^{-1}$ (determined experimentally at 37 °C), $k_{-1}$ = 0.036 $min^{-1}$, $K_2$ = 3 $\mu$M (*33*), $K_3$ = 2 $\mu$M, $k_4$ = 60 $min^{-1}$, $k_5$ = 10 $min^{-1}$, $K_6$ = 150 $\mu$M, $K_7$ = 2 $\mu$M (33), $k_8$ = 1 $min^{-1}$, $K_9$ = 50 $\mu$M, and $K_{10}$ = 8 $\mu$M (see Experimental Procedures for model). The same values were used in the other trace except that $K_2 = K_m$ = 110 $\mu$M (— · —).

at neutral or acidic pH (*20*). The increase in the $A_{340}$ of a solution of dialdehyde (in the absence of AFAR and NADPH) has been shown previously (*20*) and was repeated here, with $k$ = 1.2 $min^{-1}$ at 37 °C. In the presence of rAFAR1 and saturating NADPH, the $A_{340}$ of the reaction mixture rose and then decreased with time (Figure 8).

The change in $A_{340}$ was modeled using DYNAFIT simulation (Figure 8), because even the 15 s time points used in the HPLC analyses (Figure 7, Table 1) may yield parameters that are influenced by the nonenzymatic loss of substrate. Simplifications of the mechanism (see Experimental Procedures) include the treatment of reduction to either monoalcohol as an irreversible enzymatic reaction and the adoption of reported $K_m$ values of rAFAR1 for NADPH (*33*) as dissociation constants ($K_d$) (2 $\mu$M) for NADPH and $NADP^+$. The fits suggest that the efficiency of rAFAR1 for catalyzing the first reduction of the dialdehyde is underestimated by the $k_{cat}$ and $K_m$ in Figure 7. Fits with $K_2$ = 100 $\mu$M and $k_4$ = 12 $min^{-1}$ yielded a higher increase in $A_{340}$ (due to nonenzymatic increases in dialdehyde rearrangement) than were observed. The effective enzyme efficiency for the first step would be $(k_4 + k_5)/K_2$ = 70 $min^{-1}$/3 $\mu$M = 3 × $10^5$ $M^{-1}$ $s^{-1}$.

**Assays with Human Liver Samples.** Twelve human liver samples were used to survey the variation in AFAR activity among humans. In this preliminary study a single $AFB_1$ dialdehyde concentration of 70 $\mu$M was used with a reaction time of 60 s, using the approach of adding $AFB_1$ dialdehyde (from pH 10) to neutral buffer to start reactions. For simplicity, the amount of the monoalcohol reduction product in peak **2** was used in making estimates of activity, which is expressed on a per milligram of protein, because the monoalcohol peak **1** and $AFB_1$ dialcohol (peak **3**) were much smaller. The activities varied from 0.24 to 0.55 nmol produced/min/6 mg protein, a range of 2.3-fold (see Supporting Information).

**In Vivo Analyses.** Experiments were performed to identify and characterize the AF metabolites present in the urine of male rats following chronic administration of $AFB_1$, using HPLC and MS. Three rats were fed on a diet lacking chemopreventive antioxidants (e.g., ethoxyquin, oltipraz) and therefore the liver would not express the GST A5 subunit that would conjugate $AFB_1$ 8,9-epoxide with GSH. The livers of these animals would also express relatively low levels of rAFAR1 (*27*, *42*). $AFB_1$ dialcohol was tentatively identified in the rat urine from its $MH^+$ ion at 351.1 and a major fragment ion in MS/MS at 333.1, signifying the loss of $H_2O$.[4] An $AFB_1$ monoalcohol was also identified by its $MH^+$ ion at 349.1; however, there was not enough material to generate an MS/MS spectrum. These urinary metabolites together represent <0.01% of the daily $AFB_1$ dose.

## Discussion

The results clearly indicate that the reduction of the $AFB_1$ dialdehyde to monoalcohols proceeds more readily than with the dihydrodiol, as shown by the experiments performed at different pH values and expected from the known properties of these $AFB_1$ metabolites (*20*). $AFB_1$ dialdehyde was reduced to a mixture of the two possible monoalcohols, peaks **1** and **2** representing the C-6a and C-8 reduction products, respectively (Schemes 2 and 3, Figures 1 and 3). The C-8 reduction product appears to be preferred as the substrate for further reduction to the dialcohol (Figure 6). No major differences were found between rAFAR1 and hAFAR2.

The preferential reduction of the C-8 aldehyde group by rAFAR1 and hAFAR2 (Figure 6, Table 1) contrasts with the results of limited $NaBH_4$ reduction (Figure 5). However, with excess $NaBH_4$ the dialcohol was formed (i.e., in the work with $NaIO_4$ cleavage). The point should be made that the exact substrates for the enzymes are still not known. For instance, in Scheme 3 there are several possibilities, particularly for a reduction at the C-8 position. Further, we have used exo epoxide to generate the substrate in these studies. A chiral center exists at the C-9a position (Scheme 2). In most of the studies described here we used $AFB_1$ dialdehyde freshly generated from the epoxide in order to minimize racemization through the enol. However, we have not attempted to measure this rate[5] and do not know if the stereochemistry at C-9a influences the reductions.

The rat and human AFAR enzymes examined in the present investigation had rather similar kinetic characteristics (Table 1). A second hAFAR exists and has been cloned and expressed (*23*). Preliminary comparison of the catalytic properties of the two human reductases, done at neutral pH, suggested that hAFAR1 was less active than hAFAR2 toward $AFB_1$ dialdehyde and we did not examine it further.

[4] This experiment was done in the Johns Hopkins facility and is not directly comparable to the conditions used in the Vanderbilt facility (Figure 4D).

[5] Büchi et al. (*39*) reported on the racemization in "basic solution" as occurring "within minutes" but did not provide specific details.

**Scheme 3. Reactions of $AFB_1$ Diol (*20*) and Reductions**

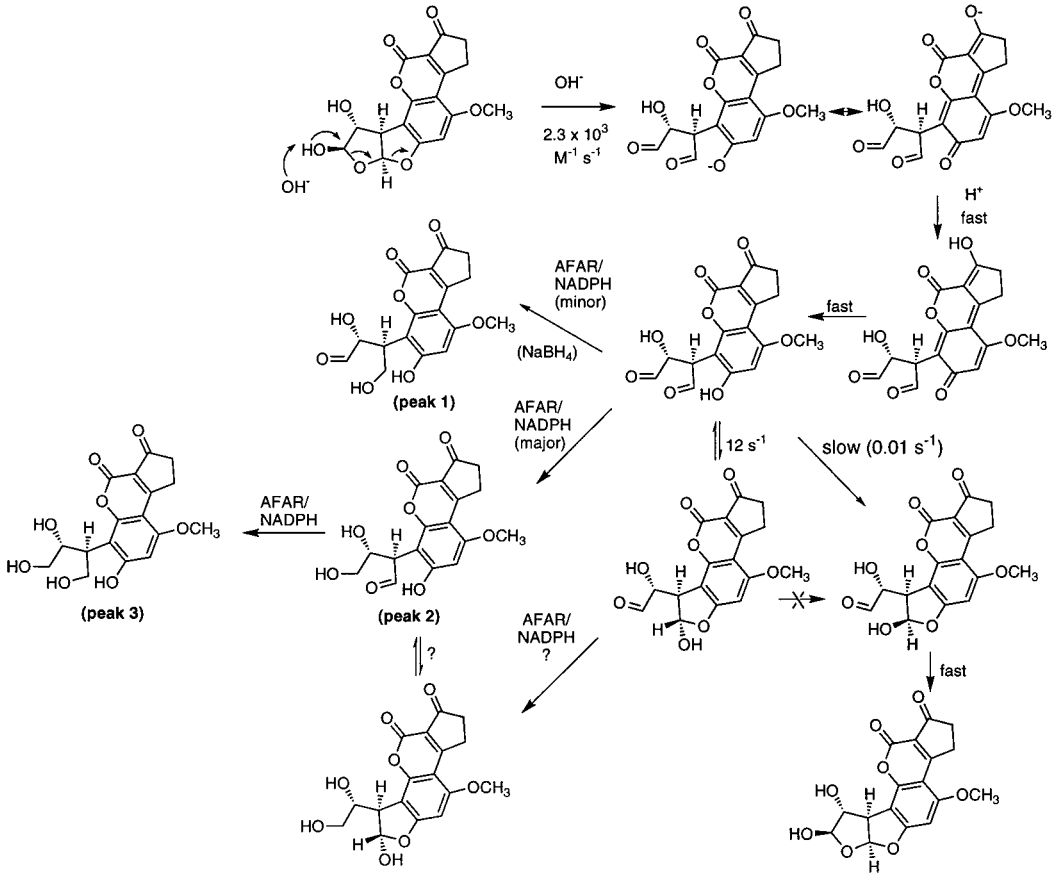


**Scheme 4. Major Steps in Human $AFB_1$ Metabolism, with Estimated Rates[a]**

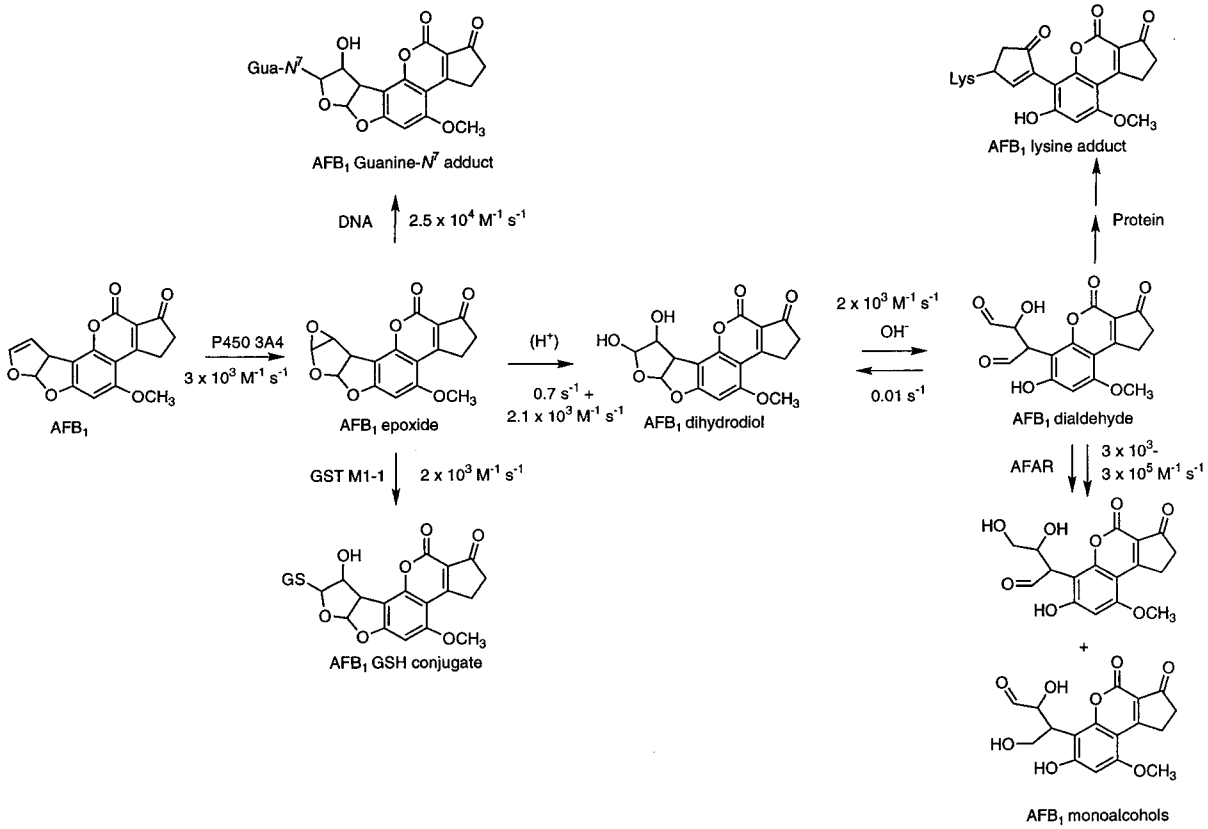


[a] Rates for individual steps are from the following references: P450 3A4 (*43*), GST M1 (*19*), DNA (*17*), epoxide hydrolysis and dihydrodiol/ dialdehyde equilibration (*20*), and hAFAR2 (Table 1, Figure 7).

The approach used here to estimate the steady-state kinetic parameters is inherently valid and gives rates for the individual products, with the caveats already presented about the stereochemistry and the possible contributions of individual isomeric structures (Scheme 3). The parameters obtained here (Table 1) suggest less efficiency of rat and human AFAR than estimated in previous studies based on NADPH oxidation (*23*, *33*). Although the HPLC assays in this present work were done with 15 s incubation time to avoid the 1.2 $min^{-1}$ rate of disappearance of $AFB_1$ dialdehyde [ref *20* and determined again at 37 °C (Figure 7)], we were concerned about the influence of the nonenzymatic changes in the substrate that occur in the course of the reaction. To address the issue, $AFB_1$ dialdehyde was added to a mixture of rAFAR1 and NADPH and $A_{340}$ was monitored as a function of time (Figure 7). A simplified model was used for the nonenzymatic and enzymatic reactions (Experimental Procedures). Even in this simplified model in which several steps are combined (e.g., see Scheme 3), there are still 10 reactions and any solutions are not exclusive. With an approximation of $K_d = 2$ $\mu$M for NADPH and $NADP^+$ (*33*), the use of the observed $k_{cat}$ for $k_4$ and $K_m$ for $K_2$ did not yield a fit the $\Delta A_{340}$ data, which is fairly stringent test in that the decrease in $A_{340}$ due to NADPH oxidation must be balanced with the increase in $A_{340}$ due to $AFB_1$ dialdehyde ring closure (Figure 8). A good fit could be made with $k_4 = 60$ $min^{-1}$, $k_5 = 10$ $min^{-1}$, and $K_2 = 3$ $\mu$M.

As indicated in the experiment described in Figure 1, rAFAR1 did not reduce the dihydrodiol. However, one possibility for reductase activity reported in previous studies (using NADPH depletion as an assay) (*23*, *33*) is that steady-state conditions were used and there is the possibility that a basic environment is provided within the active site (*1*), to convert proferred $AFB_1$ dihydrodiol to dialdehyde.

Comparing the kinetic constants of individual reaction steps in the $AFB_1$ pathway provides some concept of roles of enzymes in bioactivation and detoxication. The key reactions in Scheme 1 are presented again in Scheme 4 with nonenzymatic rates and rates for the most active human enzymes involved in the metabolism are indicated, expressed in terms of enzyme efficiency ($k_{cat}/K_m$). Some points should be made. The efficiency of the AFAR-catalyzed step is as high as those catalyzed by other enzymes, even when $k_{cat}/K_m$ (Table 1) is used. The apparent efficiency is even higher ($3 \times 10^5$ $M^{-1}$ $s^{-1}$) when $(k_4 + k_5)/K_2$ is utilized (Figure 7). The chemical equilibrium at neutral pH yields a low concentration of $AFB_1$ dialdehyde ($pK_a$ 8.2) (*20*). Nevertheless, the AFAR reaction competes directly with the reaction of the dialdehyde with proteins in the cytosol. This situation contrasts with that of the reaction of the exo epoxide with DNA, where the epoxide must move to the nucleus and the rate of DNA modification cannot be compared directly with some competing reactions (*20*). What is still missing in Scheme 4 is a rate for reaction of $AFB_1$ dialdehyde with protein.

The reduction of $AFB_1$ dialdehyde by AFAR reaction could play a significant role in attenuating the acute or even chronic toxicity of this mycotoxin. Certainly, in vitro cell-free incubations of rAFAR1 with activated $AFB_1$ have shown that the reductase can inhibit the formation of protein adducts (*24*). The contribution of AFAR to tumorigenicity is less clear. Because AFAR acts "downstream" of the ultimate carcinogenic form of $AFB_1$ (*exo*-8,9-epoxide), it is possible that the reductases could encourage the progression of neoplastic disease by protecting cells that have already acquired genetic damage. Consistent with this view, it has been reported that in rat liver AFAR is overexpressed in rat pre-neoplastic nodules caused by exposure to $AFB_1$ (*25*). However, the fact that the GSH transferase rat GST A5 subunit (previously termed $Yc_2$), which deactivates $AFB_1$ *exo*-8,9-epoxide (*19*), is also expressed in these preneoplastic nodules (*25*) suggests that both detoxication enzymes are part of a coordinately regulated adaptive response mechanism that is stimulated in initiated cells. Humans lack a GST that is as efficient as rat GST A5−5 in detoxicating $AFB_1$ *exo*-8,9-epoxide. Thus, the AFAR enzymes in man may be of more significance with regard to the overall detoxication of $AFB_1$ than the orthologous reductases in rats.

**Acknowledgment.** This work was supported in part by U.S. Public Health Service Grants R35 CA44353 (F.P.G. and H.C.), F32 ES05919 (H.C.), P30 ES00267 (F.P.G., T.M.H.), and R01 CA39416 (T.R.S.) and Grant 99-041 from the Association of International Cancer Research (J.D.H. and M.M.). We thank Melissa Mann and Bodreddigari Sideri (University Memphis) for technical assistance and Dr. William W. Johnson (Schering-Plough Research Inst.) for comments on the manuscript.

**Supporting Information Available:** Information on donor on human liver samples used in the analysis of variation in AFAR activity, plus individual values of activities. This material is available free of charge via the Internet at http://pubs.acs.org.

## References

(1) Jez, J. M., Bennet, M. J., Schlegel, B. P., Lewis, M., and Penning, T. M. (1997) Comparative anatomy of the aldo-keto reductase superfamily. *Biochem. J.* **326**, 625−636.

(2) Detroy, R. W., Lillehoj, E. B., and Ciegler, A. (1971) Aflatoxin and related compounds. In *Microbial Toxins* (Ciegler, A., Kadis, S., and Ajl, S. J., Eds.) Vol. 6, pp 3−178, Academic Press, New York.

(3) Busby, W. F., and Wogan, G. N. (1984) Aflatoxins. In *Chemical Carcinogens* (Searle, C. E., Ed.) 2nd ed., pp 945−1136, Am. Chem. Soc., Washington, DC.

(4) Groopman, J. D., Cain, L. G., and Kensler, T. W. (1988) Aflatoxin exposure in human populations: measurements and relationship to cancer. *Crit. Rev. Toxicol.* **19**, 113−145.

(5) Blount, W. P. (1961) Turkey "X" disease. *J. Br. Turkey Fed.* **9**, 52−58.

(6) Wogan, G. N., and Newberne, P. M. (1967) Dose−response characteristics of aflatoxin $B_1$ carcinogenesis in the rat. *Cancer Res.* **27**, 2370−2376.

(7) Wogan, G. N. (1992) Aflatoxins as risk factors for hepatocellular carcinoma in humans. *Cancer Res.* (Suppl. 52), 2114s−2118s.

(8) Wang, L. Y., Hatch, M., Chen, C. J., Levin, B., You, S. L., Lu, S. N., Wu, M. H., Wu, W. P., Wang, L. W., Wang, Q., Huang, G. T., Yang, P. M., Lee, H. S., and Santella, R. M. (1996) Aflatoxin exposure and risk of hepatocellular carcinoma in Taiwan. *Int. J. Cancer* **67**, 620−625.

(9) Heathcoate, J. G., and Hibbert, J. R. 1978. *Aflatoxins: Chemical and Biological Aspects*, Elsevier, New York.

(10) Zilinskas, R. A. (1997) Iraq's biological weapons. The past as future? *J. Am. Med. Assoc.* **278**, 418−424.

(11) Guengerich, F. P., and Johnson, W. W. (1999) Kinetics of hydrolysis and reaction of aflatoxin $B_1$ *exo*-8,9-epoxide and relevance to toxicity and detoxication. *Drug Metab. Rev.* **31**, 141−158.

(12) Shimada, T., and Guengerich, F. P. (1989) Evidence for cytochrome $P\text{-}450_{NF}$, the nifedipine oxidase, being the principal enzyme involved in the bioactivation of aflatoxins in human liver. *Proc. Natl. Acad. Sci. U.S.A.* **86**, 462−465.

(13) Ueng, Y.-F., Shimada, T., Yamazaki, H., and Guengerich, F. P. (1995) Oxidation of aflatoxin $B_1$ by bacterial recombinant human cytochrome P450 enzymes. *Chem. Res. Toxicol.* **8**, 218−225.
(14) Pelkonen, P., Lang, M. A., Negishi, M., Wild, C. P., and Juvonen, R. O. (1997) Interaction of aflatoxin $B_1$ with cytochrome P450 2A5 and its mutants: correlation with metabolic activation and toxicity. *Chem. Res. Toxicol.* **10**, 85−90.
(15) Eaton, D. L., and Gallagher, E. P. (1994) Mechanisms of aflatoxin carcinogenesis. *Annu. Rev. Pharmacol. Toxicol.* **34**, 135−172.
(16) Iyer, R., Coles, B., Raney, K. D., Thier, R., Guengerich, F. P., and Harris, T. M. (1994) DNA adduction by the potent carcinogen aflatoxin $B_1$: mechanistic studies. *J. Am. Chem. Soc.* **116**, 1603−1609.
(17) Johnson, W. W., and Guengerich, F. P. (1997) Reaction of aflatoxin $B_1$ *exo*-8,9-epoxide with DNA: kinetic analysis of covalent binding and DNA-induced hydrolysis. *Proc. Natl. Acad. Sci. U.S.A.* **94**, 6121−6125.
(18) Raney, K. D., Meyer, D. J., Ketterer, B., Harris, T. M., and Guengerich, F. P. (1992) Glutathione conjugation of aflatoxin $B_1$ *exo* and *endo* epoxides by rat and human glutathione S-transferases. *Chem. Res. Toxicol.* **5**, 470−478.
(19) Johnson, W. W., Ueng, Y.-F., Mannervik, B., Widersten, M., Hayes, J. D., Sherratt, P. J., Ketterer, B., and Guengerich, F. P. (1997) Conjugation of highly reactive aflatoxin $B_1$ 8,9-*exo*-epoxide catalyzed by rat and human glutathione transferases: estimation of kinetic parameters. *Biochemistry* **36**, 3056−3060.
(20) Johnson, W. W., Harris, T. M., and Guengerich, F. P. (1996) Kinetics and mechanism of hydrolysis of aflatoxin $B_1$ *exo*-8,9-oxide and rearrangement of the dihydrodiol. *J. Am. Chem. Soc.* **118**, 8213−8220.
(21) Johnson, W. W., Ueng, Y.-F., Yamazaki, H., Shimada, T., and Guengerich, F. P. (1997) Role of microsomal epoxide hydrolase in the hydrolysis of aflatoxin $B_1$ 8,9-epoxide. *Chem. Res. Toxicol.* **10**, 672−676.
(22) Sabbioni, G., Skipper, P. L., Büchi, G., and Tannenbaum, S. R. (1987) Isolation and characterization of the major serum albumin adduct formed by aflatoxin $B_1$ *in vivo* in rats. *Carcinogenesis* **8**, 819−824.
(23) Knight, L. P., Primiano, T., Groopman, J. D., Kensler, T. W., and Sutter, T. R. (1999) cDNA cloning, expression and activity of a second human aflatoxin $B_1$-metabolizing member of the aldo-keto reductase superfamily, AKR7A3. *Carcinogenesis* **20**, 1215−1223.
(24) Judah, D. J., Hayes, J. D., Yang, J.-C., Lian, L.-Y., Roberts, G. C. K., Farmer, P. B., Lamb, J. H., and Neal, G. E. (1993) A novel aldehyde reductase with activity towards a metabolite of aflatoxin $B_1$ is expressed in rat liver during carcinogenesis and following the administration of an anti-oxidant. *Biochem. J.* **292**, 13−18.
(25) Hayes, J. D., Judah, D. J., and Neal, G. E. (1993) Resistance to aflatoxin $B_1$ is associated wtih the expression of a novel aldo-keto reductase which has catalytic activity towards a cytotoxic aldehyde-containing metabolite of the toxin. *Cancer Res.* **53**, 3887−3894.
(26) Primiano, T., Gastel, J. A., Kensler, T. W., and Sutter, T. R. (1996) Isolation of cDNAs representing dithiolethione-responsive genes. *Carcinogenesis* **17**, 2297−2303.
(27) Kelly, V. P., Ireland, L. S., Elis, E. M., and Hayes, J. D. (2000) Purification from rat liver of a novel constitutively expressed member of the aldo-keto reductase 7 family that is widely distributed in extrahepatic tissues. *Biochem. J.* **348**, 389−400.
(28) Nishi, N., Shoji, H., Miyanaka, H., and Nakamura, T. (2000) Androgen-regulated expression of a novel member of the aldo-keto reductase superfamily in regrowing rat prostate. *Endocrinology* **141**, 3194−3199.
(29) Baertschi, S. W., Raney, K. D., Stone, M. P., and Harris, T. M. (1988) Preparation of the 8,9-epoxide of the mycotoxin aflatoxin $B_1$: the ultimate carcinogenic species. *J. Am. Chem. Soc.* **110**, 7929−7931.
(30) Iyer, R. S., and Harris, T. M. (1993) Preparation of aflatoxin $B_1$ 8,9-epoxide using *m*-chloroperbenzoic acid. *Chem. Res. Toxicol.* **6**, 313−316.
(31) Budavari, S., Ed. (1996) Aflatoxins B. In *The Merck Index*, 12th ed., p 33, Merck & Co., Whitehouse Station, NJ.
(32) Ellis, E. M., Judah, D. J., Neal, G. E., and Hayes, J. D. (1993) An ethoxyquin-inducible aldehyde reductase from rat liver that metabolizes aflatoxin $B_1$ defines a subfamily of aldo-keto reductases. *Proc. Natl. Acad. Sci. U.S.A.* **90**, 10350−10354.
(33) Ellis, E. M., and Hayes, J. D. (1995) Substrate specificity of an aflatoxin-metabolizing aldehyde reductase. *Biochem. J.* **312**, 535−541.
(34) Guengerich, F. P. (1994) Analysis and characterization of enzymes. In *Principles and Methods of Toxicology* (Hayes, A. W., Ed.) 3rd ed., pp 1259−1313, Raven Press, New York.
(35) Kuzmic, P. (1996) Program DYNAFIT for the analysis of enzyme kinetic data: application to HIV protease. *Anal. Biochem.* **237**, 260−273.
(36) Groopman, J. D., Trudel, L. J., Donahue, P. R., Marshak-Rothstein, A., and Wogan, G. N. (1984) High-affinity monoclonal antibodies for aflatoxins and their application to solid-phase immunoassays. *Proc. Natl. Acad. Sci. U.S.A.* **81**, 7728−7731.
(37) Nash, T. (1953) The colorimetric estimation of formaldehyde by means of the Hantzsch reaction. *Biochem. J.* **55**, 416−421.
(38) Büchi, G., Foulkes, D. M., Kurono, M., and Mitchell, G. F. (1966) The total synthesis of racemic aflatoxin $B_1$. *J. Am. Chem. Soc.* **88**, 4534−4536.
(39) Büchi, G., Foulkes, D. M., Kurono, M., Mitchell, G. F., and Schneider, R. S. (1967) The total synthesis of racemic aflatoxin $B_1$. *J. Am. Chem. Soc.* **89**, 6745−6753.
(40) Silverstein, R. M., Bassler, G. C., and Morrill, T. C. (1991) *Spectrometric Identification of Organic Compounds*, 5th ed., p 298, John Wiley & Sons, New York.
(41) McClanahan, R. H., Huitric, A. C., Pearson, P. G., Desper, J. C., and Nelson, S. D. (1988) Evidence for a cytochrome P-450 catalyzed allylic rearrangement with double bond topomerization. *J. Am. Chem. Soc.* **110**, 1979−1981.
(42) Kelly, V. P., Ellis, E. M., Manson, M. M., Chanas, S. A., Moffat, G. J., McLeod, R., Judah, D. J., Neal, G. E., and Hayes, J. D. (2000) Chemoprevention of aflatoxin B-1 hepatocarcinogenesis by coumarin, a natural benzopyrone that is a potent inducer of aflatoxin $B_1$ aldehyde reductase, the glutathione S-transferase A5 and P1 subunits, and NAD(P)H: quinone oxidoreductase in rat liver. *Cancer Res.* **60**, 957−969.
(43) Ueng, Y.-F., Kuwabara, T., Chun, Y.-J., and Guengerich, F. P. (1997) Cooperativity in oxidations catalyzed by cytochrome P450 3A4. *Biochemistry* **36**, 370−381.

TX010005P